PASJ: Publ. Astron. Soc. Japan **54**, 865–871, 2002 December 25

Development of Iodine Cells for the Subaru HDS and the Okayama HIDES: I. Instrumentation and Performance of the Spectrographs

Eiji KAMBE,[1] Bun'ei SATO,[2,3] Yoichi TAKEDA,[4] Hiroyasu ANDO,[3] Kunio NOGUCHI,[3] Wako AOKI,[3]
Hideyuki IZUMIURA,[3] Setsuko WADA,[5] Seiji MASUDA,[3] Norio OKADA, [3] Yasuhiro SHIMIZU,[3]
Etsuji WATANABE,[3] Michitoshi YOSHIDA,[3] Satoshi HONDA,[3] and Satoshi KAWANOMOTO[3]
[1]*Department of Earth and Ocean Sciences, National Defense Academy, Yokosuka, Kanagawa 239-8686*
[2]*Department of Astronomy, School of Science, The University of Tokyo, Bunkyo-ku, Tokyo 113-0033*
[3]*National Astronomical Observatory, Mitaka, Tokyo 181-8588*
[4]*Komazawa University, Komazawa, Setagaya, Tokyo 154-8525*
[5]*The University of Electro-Communications, Chofu, Tokyo 182-8585*
kambe@nda.ac.jp

(Received 2002 January 30; accepted 2002 June 26)

Abstract

We have developed iodine (I_2) cells for the High Dispersion Spectrograph (HDS) on the Subaru telescope and for the HIgh Dispersion Echelle Spectrograph (HIDES) on the Okayama 1.88 m reflector. The cell is put into a compact vacuum vessel, which fits into a small space behind the entrance slit of the HDS. The cell assembly is designed to minimize heat losses from the cell, which is heated during observations, to keep I_2 vapor from condensation. The amount of I_2 in the cell is determined to be best suited for radial-velocity measurements of solar-type stars. We also report on some performances of the HDS and HIDES as well as their instrumental profiles based on tests of our I_2 cells. Lastly, we discuss future improvements of our instruments and data-analysis softwares for I_2 observations, and also describe the scientific goals of our project.

Key words: instrumentation: spectrographs — stars: oscillations — stars: planetary systems — techniques: radial velocities

1. Introduction

Precise measurements of radial velocity of stars recently turned out to be a powerful technique in the search for extrasolar planets around stars (Mayor, Queloz 1995; Marcy, Butler 1998; Marcy et al. 2000; Butler et al. 2002) and for detecting solar-type oscillations (Bedding et al. 2001; Queloz et al. 2001). Since its discovery (Mayor, Queloz 1995), about 80 candidates of giant planets have been found so far by measuring the tiny wobble of stars in radial velocity due to the existence of planets. Extensive searches for extrasolar planets are currently on-going and/or planned around the globe (Butler et al. 2002; Cumming et al. 1999; Tinney et al. 2001; Queloz et al. 2000; Latham 2000; Nisenson et al. 1999; Cochran et al. 1999; Endl et al. 2001; Pepe et al. 2000a). Applications of precise radial-velocity measurement techniques to other astronomical objects also attract our attention, such as measuring the atmospheric motions in Cepheids (Butler 1998) and detecting very small-amplitude stellar oscillations in rapidly oscillating Ap (roAp) stars, β Cephei stars, and so on. Thus, motivated by the construction of the new echelle-type High Dispersion Spectrograph for the Subaru telescope (HDS, Noguchi et al. 1998, 2002) and of the new HIgh Dispersion Echelle Spectrograph for the Okayama 1.88 m reflector (HIDES, Izumiura 1999), we decided to develop instruments for precise measurements of the radial velocity of stars.

For such purposes, two methods, though not mutually exclusive, are extensively used in high dispersion spectroscopy at present. One is to adopt the technique of simultaneous calibration (e.g., CORALIE, Queloz et al. 2000; AFOE, Brown et al. 1994; HARPS, Pepe et al. 2000b). A stellar spectrum is usually obtained, flanked by the typical hollow-cathode lamp (Th–Ar lamp) spectra as wavelength calibration references. The merits of the technique are that the whole observed wavelength range can be used to estimate the radial velocity of stars, which might overcome the ultimate accuracy of the iodine (I_2) technique described below, and that the stellar spectrum remains uncontaminated, which facilitates its further inspection. However, to implement the simultaneous calibration capability on an existing spectrograph requires a modification of the slit area: the introduction of an image scrambler to cancel the effect of guiding errors, as well as calibration fibers adjacent to the output of the scrambler. Also, devices for object acquisition and on-slit guiding might need to be modified.

Another method is to use gas filters, like HF and I_2 (Campbell et al. 1988; Walker et al. 1995; Butler 1987; Marcy, Butler 1992). In the I_2 technique, numerous I_2 molecular absorption lines are superposed on a stellar spectrum, which can be used both as a wavelength standard and to correct for any local or time-dependent instrumental profile (IP) of a spectrograph at each position on a detector. It is in fact a merit of the I_2 technique that we can essentially compensate for changes of IP due to guiding errors or distortions of the spectrographs. The I_2 cell can be added to existing spectrographs without many modifications to them. Since both spectrographs were in the final stage of construction when we started our precise radial-velocity measurement project, we decided to introduce I_2 cells.

In section 2, we describe our newly developed I_2 cells for HDS and HIDES. We present some performances of both spectrographs examined by the I_2 technique in section 3. Lastly, in section 4, we describe the scientific goals of our project and discuss future improvements of the instruments and data-analysis softwares for I_2 observations. The development of data-analysis softwares for the I_2 technique and results concerning the accuracy of a radial-velocity measurement with our I_2 cells are extensively discussed in Sato et al. (2002, hereafter Paper II).

2. Development of New Iodine Cells

When we decided to make the I_2 cell for the HDS, a pilot project of "precise detection of very small radial velocity variation" had already been started at Okayama, anticipating completion of HIDES, in which the proto-type cell was installed and had been tested (Takeda et al. 2002).

A few drawbacks of the proto-type I_2 cell were noticed and rectified during the development of the new I_2 cell for HDS. Since the same design was adopted for the new cells for both spectrographs, we mainly describe the new I_2 cell for HDS in the following subsections.

2.1. *Amount of I_2*

The amount of I_2 put into the proto-type cell was much larger than the optimum one. Thus, the depth of the I_2 absorption lines is rather controlled by the temperature of the cell kept at about 50℃ by a thermo-controller with an accuracy of ±1℃ (Takeda et al. 2002). Under such a condition, however, the precision of the radial-velocity measurement may be limited, since the depths of the I_2 lines vary from observation to observation. Some I_2, once vaporized, also re-condenses onto the cold part of the surface windows of the cell, thus hindering stellar light from traveling further into the spectrograph.

In order to prevent such undesirable situations to occur, we tried to enclose the optimum amount of I_2 in the new cells so that we could measure the radial velocity of stars as precisely as possible. Such an amount definitely depends on the resolution of the spectrograph, and the types and rotational velocities of the observed stars. Here, we use the solar spectrum to estimate the optimum amount of I_2, since planet searches around G-type stars and the detection of solar-type oscillations are the main scientific purposes of our project (see section 4). To simulate an observed stellar spectrum superposed by an I_2 spectrum (star + I_2 spectrum), we first multiply the normalized very high-resolution solar spectrum (Delbouille et al. 1990) by the very high-resolution Lick I_2 spectrum (kindly provided by G. W. Marcy) with a modification of the line depth, depending on the amount of I_2, by simply multiplying a constant value to its depth. Then, we convolve the resultant spectrum by a Gaussian profile corresponding to the resolution of the spectrograph ($R = 100000$ for HDS). Lastly, we rebin the spectrum into the typical sampling interval of our spectrograph ($\delta\lambda = 0.018$ Å for HDS).

As an estimate of the accuracy of determining the I_2 spectrum position on a detector, we use (Butler et al. 1996)

$$\delta v_{\mathrm{I}_2} = \frac{1}{\sqrt{\sum_i \frac{1}{\delta v_i^2}}} = \frac{1}{\sqrt{\sum_i \left[\frac{\lambda}{c}\frac{(l_{\mathrm{I}_2,i+1} - l_{\mathrm{I}_2,i})}{\Delta\lambda}\sqrt{N}\right]^2}}, \quad (1)$$

where l_{I_2} is the line depth relative to the continuum level and $\Delta\lambda$ is the sampling interval. The continuum level of the I_2 (and also the star + I_2) spectra, N, is set to $10^5 \mathrm{e}^-$ pixel^{-1}, which can be attained by one exposure. The summation in the equation is taken over all data points between 5150 Å and 5700 Å, where the I_2 absorption lines are deep and sharp. By substituting $l_\odot$ for l_{I_2}, we can calculate the ultimate accuracy of measuring the radial velocity of the solar-type stars, that is about 70 cm s^{-1} per exposure for HDS, provided that its reciprocal resolution is about 100000 (corresponding to three pixels). The accuracy for HIDES is slightly lower because of the lower resolution of the spectrograph.

The δv_{I_2} becomes smaller until the I_2 absorption lines become considerably deeper. However, the accuracy of determining the stellar spectrum position relative to that of I_2 should decrease with increasing depth of the I_2 absorption lines. Thus, as an indicator for the accuracy, we introduce

$$\delta v_{\odot,\mathrm{eff}} = \left(\frac{1}{\delta v_{\odot+\mathrm{I}_2}^2} - \frac{1}{\delta v_{\mathrm{I}_2}^2}\right)^{-1/2}, \quad (2)$$

where $\delta v_{\odot+\mathrm{I}_2}$ is obtained by substituting $l_{\odot+\mathrm{I}_2}$ for l_{I_2} in equation (1). The $\delta v_{\odot+\mathrm{I}_2}$ shows a potential ability for determining the positions of I_2 and the stellar lines from the star + I_2 spectrum. In figure 1, we show how δv_{I_2} and $\delta v_{\odot,\mathrm{eff}}$ change with the equivalent widths of the I_2 absorption lines for HDS. In the figure, the equivalent width is shown relative to that of the Lick I_2 spectrum.

We choose the optimum amount of I_2 molecules so that $\delta v = [(\delta v_{\mathrm{I}_2})^2 + (\delta v_{\odot,\mathrm{eff}})^2]^{1/2}$ is minimized. The equivalent width of the resultant I_2 absorption line thus estimated for HDS is by about 40% shallower than that of the Lick I_2 spectrum (see also subsubsection 2.2.1). This difference may be partly due to the specifications of the spectrographs, and partly due to the fact that we did not take into account that δv_{I_2} could also be degraded in the star + I_2 spectrum. The ambiguity in determining a continuum level of the star + I_2 spectrum, which increases with the I_2 line depth, might also lower the accuracy of the radial-velocity measurement. In any case, the estimated accuracy of measuring the radial velocity of solar-type stars is about 1.1 m s^{-1} per exposure for HDS and 1.7 m s^{-1} per exposure for HIDES.

2.2. *Iodine Cell Assembly*

In developing the new I_2 cells for HDS, there are a few important points we must pay attention to. The whole I_2 cell assembly should fit into a very small space (10 cm length × 20 cm width × 20 cm height) at a location 50 cm behind the entrance slit of HDS and just under its echelle grating, which was the only space available for the I_2 cell near to the slit. The assembly includes a heater which vaporizes the I_2 molecules during observations, an insulator which thermally separates the cell from the rest of the spectrograph, and a driving mechanism which moves the cell in and out of the optical path.

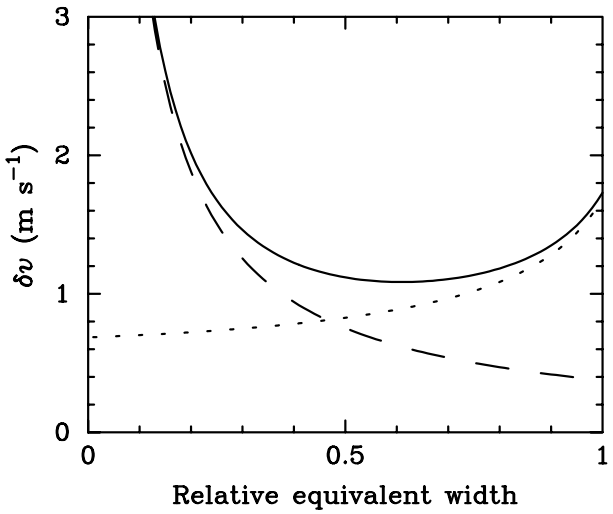

Fig. 1. Accuracy of a radial-velocity measurement as a function of the equivalent widths of the I_2 absorption lines. It is shown as the relative equivalent width to that of the Lick I_2 spectrum. The solid line is for δv, the dashed line is for δv_{I_2}, and the dotted line is for $\delta v_{\odot,\mathrm{eff}}$.

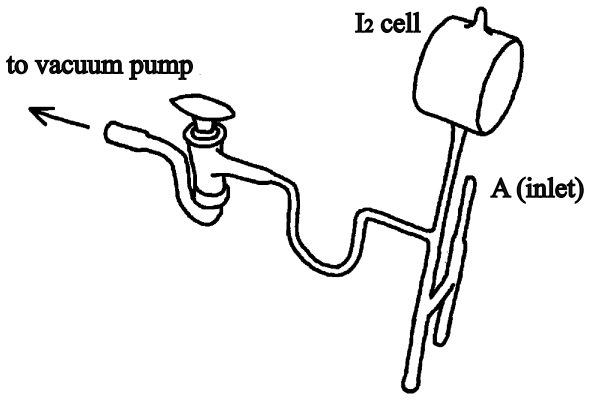

Fig. 2. Glass assembly for enclosing I_2 in the cell. The tip of the tube, indicated by A, is used as an inlet.

2.2.1. Newly developed I_2 cells

Since the space available for the cell is very restricted for HDS, we use a Pyrex cylindrical cell with a diameter of 55 mm and a length of 38 mm, including two optical side windows with 4 mm thickness each. The beam diameter for a point source at the position of the cell is about 38 mm.

We have applied anti-reflection coatings on both surfaces of the optical windows to maximize their transparency. Multiple-layer coatings are applied to the outer surfaces of the cell, while single-layer coatings with diameters of about 44 mm are applied to the inner surfaces of the cell, since the multiple-layer coating is not immune to the high temperature at which the windows are melt-sealed to the cylindrical body.

To enclose I_2 in the cell, we first made a glass assembly, as shown in figure 2. Two straight tubes, long and short ones, were puncture-melted at the opposite sides of the cylindrical body of the cell. The shorter tube projected above the cell is about 10 mm length, the end of which is flame-pinched by a gas blower. The end of the long tube is also flame-pinched. Anothor two tubes are branched off at around the center of the long tube: a T-shaped tube with all ends closed as an inlet for I_2 (the shape is not so important), and a valve-attached tube as an interface to a vacuum pump. Before introduction of I_2, we evacuated the glass assembly, warming it up by a hair dryer. After removing it from the vacuum pump, we cut open one end of the T-shaped tube (marked as A in figure 2) and circulated dry (Argon) gas through the glass assembly.

We weighed an appropriate amount of solid I_2 (about 1.4 mg for HDS) carefully, inserted it into the glass assembly from the inlet, and rolled it to the end of the long tube. Then, the inlet was flame-pinched and the assembly was re-connected to the vacuum pump. After dipping the end of the long tube in liquid nitrogen, we started the pump. By keeping the temperature of I_2 much lower than the freezing point, little I_2 vaporized while pumping. After the glass assembly was well evacuated, we flame-pinched off the T-shaped tube and the valve-attached tube. Lastly, we re-condensed the I_2 inside the assembly at the tip of the short tube by dipping the tube in liquid-nitrogen, and then cut off the long tube.

The amount of I_2 in the cell for HDS is by 30% more than the optimum amount of I_2 we estimate in subsection 2.1. This is simply because we were too much afraid of losing I_2 during our enclosing process. We chose to enclose more I_2 rather than less I_2 in the cell, since from our simulation it would not degrade the accuracy of radial-velocity measurement much. The amount of I_2 in the cell for HIDES, which was manufactured later, differs only by several percent from the optimum amount of I_2 which we estimated. The optical depth of the cell for HDS is about 80% of the Lick Iodine cell (Marcy, Butler 1992). Since the length of our cell (30 mm) is shorter than that of the Lick Iodine cell (100 mm), the partial vapor pressure of our cell (about 2 mmHg) is higher than that of Lick's. Thus, to keep the molecular iodine vaporized sufficiently during observations, we require a higher operation temperature (at least 49 ℃) than that for the Lick Iodine cell. After taking flat + I_2 spectra at various operating temperatures, we chose the operation temperature to be 55 ℃, around which depths and equivalent widths of the I_2 lines change little with temperature.

2.2.2. Other features of the I_2 cell assembly

To maximize the efficiency of heating the I_2 cell, we put the cell in a vacuum vessel (figures 3 and 4). The cell is covered with a copper cylinder, around which a stainless-steel sheath heater is melt-wound. The side of the cell is cushioned by woolly copper-made cloth and thin copper sheets for better thermal conductivity between the cell and the copper cylinder. Then, the copper cylinder is hung with two stainless-steel Y-shaped supporters from an epoxy plate attached inside a brass lid of the small vacuum vessel. We also covered the copper cylinder with a stainless-steel radiation shield, which later turned out to increase the heat efficiency considerably. With a moderate degree of vacuum inside the vessel, 5 W is sufficient to keep the cell warm enough, even under an ambient temperature of around 0 ℃.

The vacuum vessel has a detachable valve for pumping. For HDS a concave lens is used as one of the windows of the vacuum vessel so as to compensate for the shift of the focal plane

Fig. 3. I_2 cell, a copper cylinder, a radiation shield, a vacuum vessel, and so on.

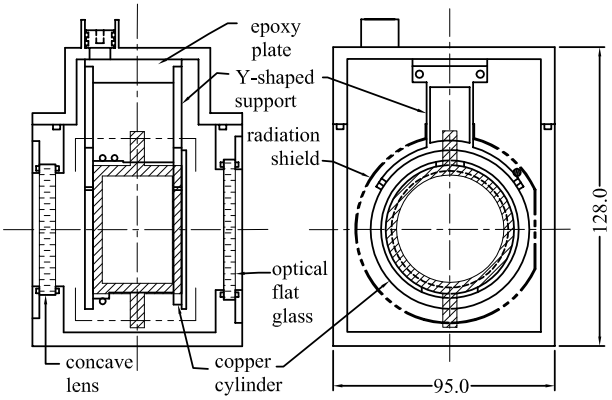

Fig. 4. Cross-sectional drawings of the vacuum vessel for HDS. The shape of the I_2 cell is hatched with oblique lines. A filled circle in the right figure is the position used for the temperature control of the cell.

position caused by the windows of the cell in the optical path. This, however, may also cause shifts of the spectral format by inserting the cell in the beam. From our test, it is about 0.01 Å (0.5 pixel) in the dispersion direction and about two pixels in the perpendicular direction. The focal plane position is not completely compensated for, and still shifts by about 90 μm. The windows of the vacuum vessel for HIDES are optically flat Pyrex glass, because it is placed before the entrance slit of the spectrograph.

We control the cell temperature by monitoring the temperature near the copper cylinder (see figure 4). According to our test, the temperature of the copper cylinder is kept stable within ± 0.4 ℃ and the temperature at the bump of the cell does not change by more than ± 0.2 ℃. At an operation temperature of 55 °C, we do not detect any significant change in the depths and equivalent widths of the I_2 absorption lines.

A very small 9-pin connector, which is normally used for a vacuum tube, was welded onto the top of the vacuum vessel, and used for connecting electronic wires inside and outside of the vessel. Finally, the vacuum vessel is set on a short stage to move it remotely between on-axis and off-axis positions.

3. Tests of New Cells and Some Performances of HDS and HIDES

In this section, we report on some performances of the new spectrographs, which were examined with our I_2 cells. The stability of the spectrographs against ambient environmental fluctuations, as well as shapes of instrumental profile (IP), is our concern here. In fact, various improvements have been made during the course of our project for increasing the stability of HIDES (see below).

3.1. Stability of the Spectrographs

To examine how the spectrographs could be stable during observations, we monitored the positions of the I_2 spectra on the CCD during tests of our I_2 cells. The temperature inside the spectrographs, which is one of major environmental elements for their stability, was also monitored during the tests. The I_2 spectra were obtained by observing an incandescent lamp penetrating the I_2 cell.

An apparent shift of the I_2 spectrum relative to a template spectrum, which is normally the first exposure of a run, was calculated in the following manner. We first divided the echelle format spectrum into segments with widths of about 5 Å, and then calculate the radial-velocity difference of each segment between two spectra by fitting a Gaussian profile to the cross-correlation function of corresponding two spectrum chunks. Then, the spectrum shift between two exposures was estimated by averaging the radial-velocity shifts of the individual 5 Å segments over a region where the I_2 absorption lines were moderately strong.

In figure 5, we show histograms of the radial-velocity shifts of individual 5 Å segments for three I_2 spectra relative to a template spectrum. The spectra were obtained during a test run of HDS on 2000 July 3. Two exposures separate about 0.5 hours at the top panel and five hours at the bottom panel in the figure. Since the change of IP was not taken into account in our current analysis, the ideal precision of the radial-velocity measurement may be estimated when the IP's are almost the same between two spectra. This corresponds to the top panel of the figure 5. In this case, the rms spread in the radial-velocity shifts of the individual 5 Å segments is about 6 m s^{-1}. Because the number of segments is more than 100, the relative position of the two spectra can be determined with a precision of less than 1 m s^{-1}. This agrees with the theoretical expectations (subsection 2.1).

On the other hand, drifts of the spectrograph of about 10 m s^{-1} sometimes occurs even within a short exposure of 10 s. So far, we have not identified the causes of this short-term instability. The vacuum vessel, itself, the temperature of which is by about 10 ℃ higher than the ambient temperature, seems to be the only heat source inside HDS that could degrade "instrumental seeing" during observations. To specify the culprit, however, extensive monitoring of the temperatures at various locations inside the HDS room as well as the ambient pressure are necessary, because the HDS room is thermally insulated only passively. We have also noticed that the rms spread in the radial velocity results from the individual segments increases with the radial-velocity difference of two spectra, indicating that compensations for the differences of IP's are crucial in such cases.

In figure 6, we plot how the I_2 spectrum shifts in velocity unit

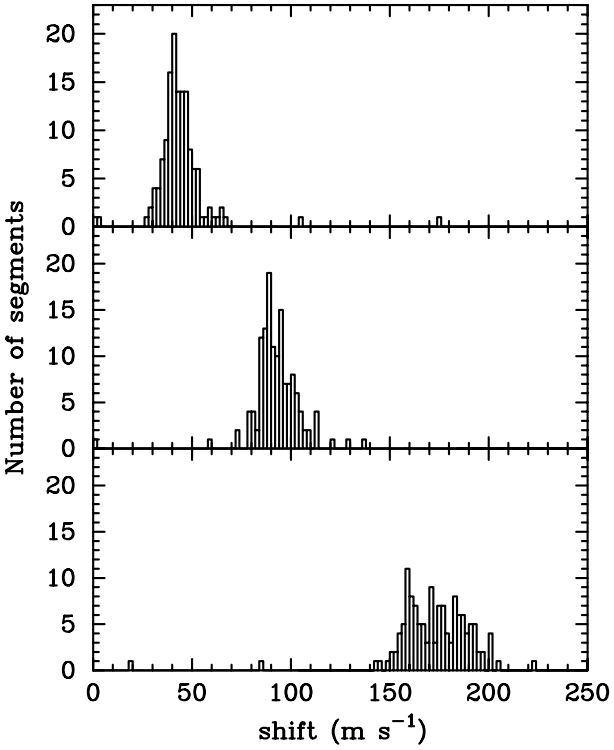

Fig. 5. Histogram of the radial-velocity shifts of individual 5 Å segments between an I_2 spectrum and a template spectrum. See text for details.

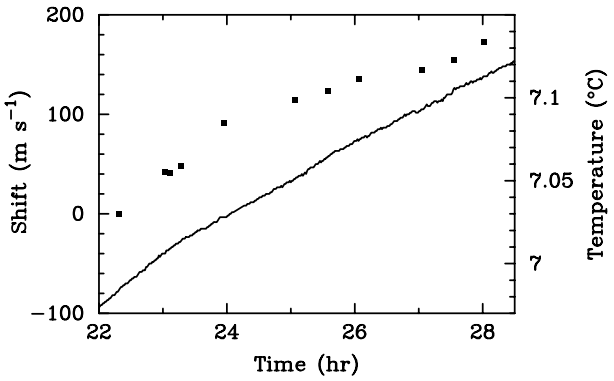

Fig. 6. Shifts of the I_2 spectra on the CCD during a test observing night, 2000 July 3. The temperature inside HDS is also shown as the solid line.

for HDS over several hours. The temperature near the echelle grating was monitored and is also shown in the same figure. In this case, the spectrum position drifts rather smoothly, depending on the temperature, with a gradient of $135\,\mathrm{m\,s^{-1}}/0.^{\circ}1\mathrm{C}$. The temperature inside the HDS room, which is thermally insulated from the outside, was stable within $0.^{\circ}1\mathrm{C}$ during the night.[1]

On the other hand, the temperature sensitivity of HIDES turned out to be much larger than that of HDS, and its gradient was about $1000\,\mathrm{m\,s^{-1}}/0.^{\circ}1\mathrm{C}$. What is worse, the I_2 spectrum position sometime changed intermittently by an amount of $500\,\mathrm{m\,s^{-1}}$. After realizing these facts, we introduced a better air-conditioner for the coudé room as well as a remote operation system of HIDES, which made it unnecessary to enter the coudé room during observing runs.

3.2. Instrumental Profiles of Spectrographs

To measure the radial velocity of stars precisely down to a level of a few $\mathrm{m\,s^{-1}}$, it is indispensable to make a correction for IP that depends on the position of the CCD, and also varies from exposure to exposure (Valenti et al. 1995; Butler et al. 1996; Endl et al. 2000). For this purpose, we currently develop computer codes to model the observed star + I_2 spectrum and IP from templates of the very high-resolution I_2 and a stellar spectrum (Paper II). In this work, we used Sato's code to model the I_2 (flat + I_2) spectrum and IP's of the spectrographs. The method is similar to that of the Lick group (Valenti et al. 1995; Butler et al. 1996) because IP is modeled with a central Gaussian profile flanked by several Gaussian satellites. The IP was determined by the least-squares fitting of the flat + I_2 spectrum to the high-resolution I_2 spectrum convolved with the modeled IP. In our model, ten Gaussian satellites were placed at the same interval of about one pixel and their Gaussian widths are set to be 0.9 pixel. The heights of Gaussian satellites relative to that of the central Gaussian profile were determined as free parameters. A more detailed modeling technique as well as its current limitations will be described in Paper II.

In figures 7–10, we show examples of IP's at various positions of the detectors for HDS and HIDES. The width of each segment is set to about 5 Å. The flat + I_2 spectra used here were obtained on 2000 July 3 for HDS, and on 2000 December 25 for HIDES, respectively. The slit widths correspond to three pixels in these exposures.

The width and height of IP for HDS varies non-monotonicly along with the wavelength in a single echelle order. The wavelength scale also shows a similar pattern in the case of HDS.

In these examples, IP's of HDS are rather symmetric and close to the Gaussian profile, while those of HIDES are more or less box-shaped. The IP of HDS and HIDES will be examined more extensively in Paper II and by Noguchi et al. (2002). When IP is not symmetric, careful modeling of IP is very important for a precise measurement of the radial velocity of stars.

4. Summary and Discussion

We have developed the I_2 cell for HDS and HIDES. We tried to enclose the optimum amount of I_2 in the cell for the radial-velocity measurement of solar-type stars. The I_2 cell assembly is designed to fit to the small space available inside HDS, pursuing the highest stability of the I_2 line profile. Our analysis shows that with our newly developed cell the relative position of the I_2 spectra on the detector can be determined with an accuracy of $1\,\mathrm{m\,s^{-1}}$ or less for HDS, as reported in subsection 3.1.

4.1. Future Improvements

In addition to the I_2 cell, we have also developed photon monitors both for HDS and HIDES to determine an effective center of the exposure time, which is important to make a correction for the Earth's motion. It is a simple system that

[1] The temperature change of HDS room is typically $0.^{\circ}1\mathrm{C\,hr^{-1}}$.

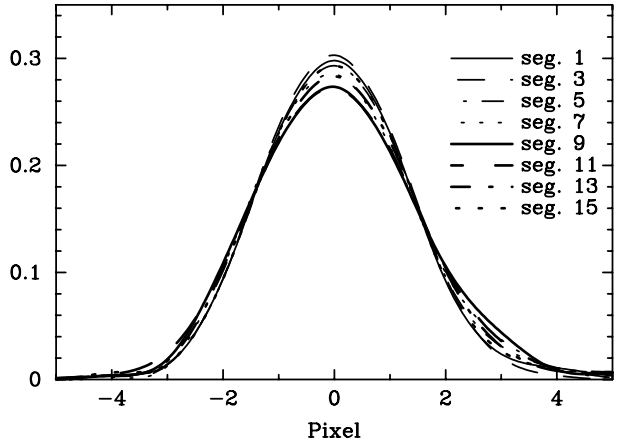

Fig. 7. IP of HDS estimated from the flat + I_2 spectrum. The IP at an echelle order (center wavelength is 573.0 nm) gradually changes along the wavelength (CCD line).

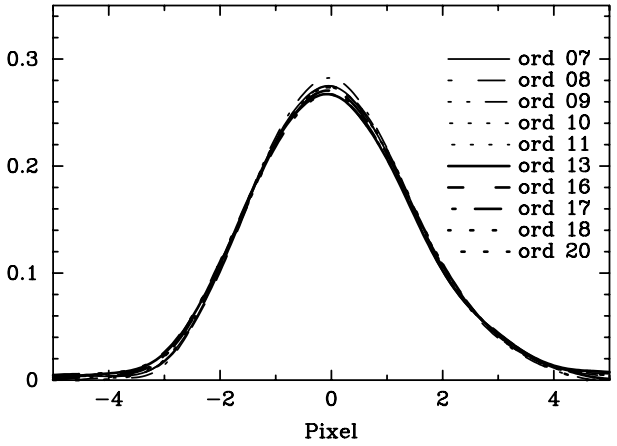

Fig. 8. Same as figure 7, but the IP near the center column of the CCD is plotted for various echelle orders. The IP is similar over orders.

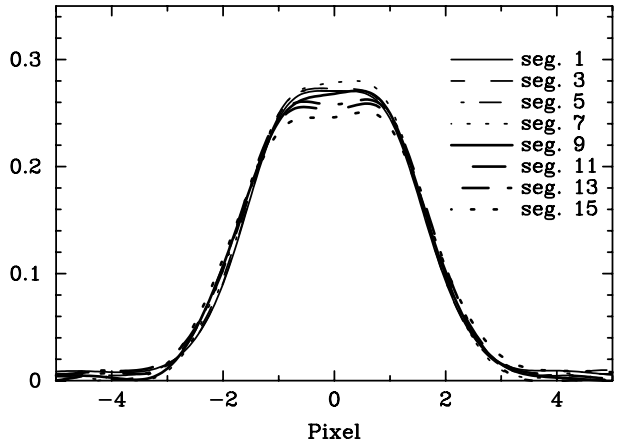

Fig. 9. IP of HIDES estimated from the flat + I_2 spectrum. The IP at an echelle order (center wavelength is 557.8 nm) is shown along the wavelength (CCD line). The IP of HIDES is asymmetric and box-shaped if the slit width corresponds to three pixels.

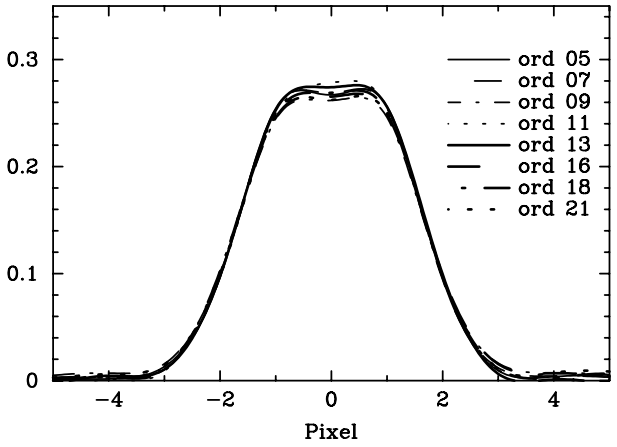

Fig. 10. Same as figure 9, but the IP near the center column of the CCD is plotted for various echelle orders.

consists of a thin dichroic mirror which introduces about 1% of the incident light to a photon monitor, a Fabry lens, and a photo-multiplier. Preliminary results of our test observations show that it can monitor the number of photons penetrating the entrance slit of the spectrograph within at least an accuracy of 1%.

The IP's of both HDS and HIDES are expected to be more or less box-shaped and/or asymmetric when spectra are taken with the typical slit widths. Thus, to determine the radial velocity of stars precisely, corrections for the position- and time-dependent IP's of the spectrographs are the next crucial step. Most of our efforts are now focused on the development of computer codes to model the observed star + I_2 spectra and IP's of spectrographs. We have already reported to have reached an accuracy of 10–15 m s^{-1} for HIDES based on one-week-long test observations of υ And (Takeda et al. 2002). In Paper II, we examine the accuracy of the radial-velocity measurement with our I_2 cells extensively from week-, month-, and even year-long observations of solar-type radial velocity standard stars.

A collimated beam is variable with the time and hour angle of the telescope, which may limit the accuracy of a radial-velocity measurement. To suppress this effect, collimator masks are often installed with I_2 cells at other observatories. We also made such masks recently, and plan to test to what extent they help to improve the precision of radial-velocity measurement.

4.2. Scientific Goals

We currently have two main scientific goals of our I_2 observations. One is to search for extra-solar planets around stars; the other is to detect radial and nonradial oscillations of various type of stars for asteroseismology.

For the former subject, we would focus on planet searches around a homogeneous type of stars. With the completion of our new I_2 cells, we have started a planet survey around G giants, the environments around which are much different from those of solar-type stars, and may give us a clue to understand the formation mechanism of planets (B. Sato et al.,

in preparation). Stars in clusters are other fascinating targets to search for extra-solar planets.

We also plan, and have tried, to observe stellar oscillations in some types of stars, including solar-type oscillations, β Cephei stars, and roAp stars. With the unique longitudinal location of Okayama on the globe, it may be one of the important observing sites for asteroseismological studies.

We are grateful to the members of the Advanced Technology Center of National Astronomical Observatory for their support in manufacturing the I_2 cell assembly. We thank for staff members at the Subaru telescope and the Okayama Astrophysical Observatory for their help during the installation of the I_2 cells. E. K. would also like to thank Drs. Hideaki Miyazaki, R. Paul Butler, and Morikazu Hosoe for their advice during the manufacturing of the I_2 cells.

References

Bedding, T. R., Butler, R. P., Kjeldsen, H., Baldry, I. K., O'Toole, S. J., Tinney, C. G., Marcy, G. W., Kienzle, F., & Carrier, F. 2001, ApJ, 549, L105

Brown, T. M., Noyes, R. W., Nisenson, P., Korzennik, S. G., & Horner, S. 1994, PASP, 106, 1285

utler, R. P. 1987, Master Thesis, San Fransisco State University

Butler, R. P. 1998, in ASP Conf. Ser., 135, A Half Century of Stellar Pulsation Interpretations, ed. P. A. Bradley & J. A. Guzik (San Francisco: ASP), 201

Butler, R. P., Marcy, G. W., Fischer, D. A., Vogt, S. S., Tinney, C. G., Jones, H. R. A., Penny, A. J., & Apps, K. 2002, in ASP Conf. Ser., Planetary Systems in the Universe: Observation, Formation and Evolution, ed. A. Penny, P. Artymowics, A.-M. Lagrange, & S. Russels (San Francisco: ASP) in press

Butler, R. P., Marcy, G. W., Williams, E., McCarthy, C., Dosanjh, P, & Vogt, S. S. 1996, PASP, 108, 500

Campbell, B., Walker, G. A. H., & Yang, S. 1988, ApJ, 331, 902

Cochran, W. D., & Hatzes, A. P. 1999, in ASP Conf. Ser., 185, Presice Stellar Velocities, ed. J. B. Hearnshaw & C. D. Scarfe (San Francisco: ASP), 113

Cumming, A., Marcy, G. W., & Butler, R. P. 1999, ApJ, 526, 890

Delbouille, L., Roland, G, & Neven, L. 1990, Atlas photometrique du spectre solaire de λ 3000 Å à λ 10000 Å (Liège: Université de Liège, Institut d'Astrophysique) ⟨http://mesola.obspm.fr/present_en.html⟩

Endl, M., Kürster, M., & Els, S. 2000, A&A, 362, 585

Endl, M., Kürster, M., Els, S., Hatzes, A. P., & Cochran, W. D. 2001, A&A, 374, 675

Izumiura, H. 1999, in Proc. 4th East Asian Meeting on Astronomy, ed. P. S. Chen (Kunming: Yunnan Observatory), 77

Latham, D. W. 2000, in ASP. Conf. Ser., 219, Disks, Planetesimals, and Planets, ed. F. Garzon, C. Eiroa, D. de Winter, & T. J. Mahoney (San Francisco: ASP), 596

Marcy, G. W., & Butler, R. P. 1992, PASP, 104, 270

Marcy, G. W., & Butler, R. P. 1998, ARA&A, 36, 57

Marcy, G. W., Cochran, W. D., & Mayor, M. 2000, in Protostars and Planets IV, ed. V. Mannings, A. P. Boss, & S. S. Russell (Tucson: University Arizona Press), 1285

Mayor, M, & Queloz, D. 1995, Nature, 378, 355

Nisenson, P., Contos, A., Korzennik, S., Noyes, R., & Brown, T. 1999, in ASP Conf. Ser., 185, Precise Stellar Velocities, ed. J. B. Hearnshaw & C. D. Scarfe (San Francisco: ASP), 143

Noguchi, K., Ando, H., Izumiura, H., Kawanomoto, S., Tanaka, W., & Aoki, W. 1998, Proc. SPIE, 3355, 354

Noguchi, K., Aoki, W., Kawanomoto, S., Ando, H., Honda, S., Izumiura, H., Kambe, E., Okita, K., et al. 2002, PASJ, 54, 855

Pepe, F., Mayor, M., Benz, W., Bertaux, J.-L., Sivan, J.-P., Queloz, D., & Udry, S. 2000a, in From Extrasolar Planets to Cosmology: The VLT Opening Symposium, ed. J. Bergeron & A. Renzini (Berlin: Springer-Verlag), 572

Pepe, F., Mayor, M., Delabre, B., Kohler, D., Lacroix, D., Queloz, D., Udry, S., Benz, W., Bertaux, J.-L., & Sivan, J.-P. 2000b, Proc. SPIE, 4008, 582

Queloz, D., Mayor, M., Naef, D., Santos, N., Udry, S., Burnet, M., & Confino, B. 2000, in From Extrasolar Planets to Cosmology: The VLT Opening Symposium, ed. J. Bergeron & A. Renzini (Berlin: Springer-Verlag), 548

Queloz, D., Mayor, M., Udry, S., Burnet, M., Carrier, F., Eggenberger, A., Naef, D., Santos, N., et al. 2001, Messenger, 105, 1

Sato, B., Kambe, E., Takeda, Y., Izumiura, H., Ando, H. 2002, PASJ, 54, 873 (Paper II)

Takeda, Y., Sato, B., Kambe, E., Watanabe, E., Miyazaki, H., Wada, S., Ando, H., Masuda, S., et al. 2002, PASJ, 54, 113

Tinney, C. G., Butler, R. P., Marcy. G. W., Jones, H. R. A., Penny, A. J., Vogt, S. S., Apps, K., & Henry, G. W. 2001, ApJ, 551, 507

Valenti, J. A., Butler, R. P., & Marcy, G. W. 1995, PASP, 107, 966

Walker, G. A. H., Walker, A. R., Irwin, A. W., Larson, A. M., Yang, S. L. S., & Richardson, D. C. 1995, Icarus, 116, 359